A computational model of orientation-dependent activation of retinal ganglion cells

Timothy Esler[1,#], Anthony N. Burkitt[1], David B. Grayden[1], Robert R. Kerr[2], Bahman Tahayori[3], Hamish Meffin[4]

Abstract— **Currently, a challenge in electrical stimulation for epiretinal prostheses is the avoidance of stimulation of axons of passage in the nerve fiber layer that originate from distant regions of the ganglion cell layer. A computational model of extracellular stimulation that captures the effect of neurite orientation in anisotropic tissue is developed using a modified version of the standard volume conductor model, known as the cellular composite model, embedded in a four layer model of the retina. Simulations are conducted to investigate the interaction of neural tissue orientation, electrode placement, and stimulation pulse duration and amplitude. Using appropriate multiple electrode configurations and higher frequency stimulation, preferential activation of the axon initial segment is shown to be possible for a range of realistic electrode-retina separation distances. These results establish a quantitative relationship between the time-course of stimulation and physical properties of the tissue, such as fiber orientation.**

I. Introduction

The retinotopic organization of retinal neural cells with respect to incident light is preserved throughout the outer retina and in retinal ganglion cells (RGC) in the ganglion cell layer (GCL), but is lost in the nerve fiber layer (NFL) as ganglion cell axons traverse the surface of the retina toward the optic disk. As a result of this organization, epiretinal electrical stimulation faces the challenge of stimulating the deeper, retinotopically-organized GCL whilst minimizing activation of axons of passage (AOP) in the NFL. Commonly, visual percept shapes described by recipients of epiretinal implants are irregular due to stimulation of axons of passage, significantly limiting perceptual efficacy [1-4]. This effect has been confirmed both experimentally and in simulations, and results in a reduction in the spatial selectivity of epiretinal stimulation [1-6].

The aim of this research is to explore the effect of axon orientation, electric field orientation and stimulation parameters on RGC activation. We use a computational modeling approach to show how the inherent distribution of neurite orientations in the GCL and NFL has an influence on their activation. Specifically, the direction of overlying passing axon tracts represents the dominant fiber orientation in a given location in the NFL. These axons are packed together as largely parallel fibers. In contrast, proximal axon regions such as the axon initial segment (AIS), located in the GCL, have a wider distribution of orientations as they pass out from the soma. Further, we will show how these differences, in combination with knowledge of differences in membrane threshold potential at the high-density sodium channel band (SOCB) and the distal axon, can be utilized to target specific neuronal structures, and suggest strategies for more targeted stimulation of retinal volumes.

In this work, we model extracellular stimulation with a four layer approximation of the retina, including layers for an insulator backing, the vitreous humor, the NFL, and the GCL (Fig. 1). Current flow and passive neural activation are modeled using a modified version of the standard volume conductor, the cellular composite model, first described by Meffin et al. [7-10]. This framework addresses a number of limitations of conventional volume conductor models, by capturing the spatiotemporal properties of neural tissue, thus allowing for an accurate analysis of the dependencies between stimulation frequency, electrode-neurite separation and neurite orientation. In order to capture the effects of both electric field and neurite orientation, the model has been generalized to allow for the analysis of multiple disk electrodes and axons of arbitrary orientation.

II. Methods

A. Volume conductor models

Volume conductor models describe extracellular electrical stimulation using a two-stage approach. The first stage models the extracellular electric field induced by the stimulating electrodes using a continuous, macroscopic approximation of the tissue. The second stage takes the

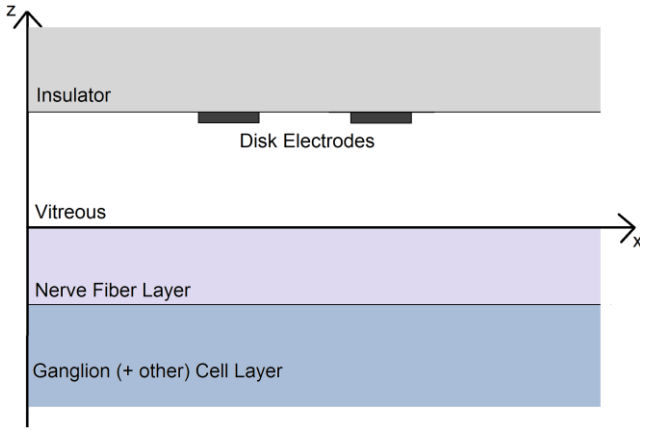

Figure 1: Geometry of the four layer model of the retina, showing each layer: the insulator (glass), vitreous, NFL and GCL. For simplicity, the insulator and GCL are assumed to have infinite extent in the z-direction.

[1]NeuroEngineering Laboratory, Dept. of Electrical and Electronic Engineering, University of Melbourne. [2]IBM Research Australia, Melbourne. [3]Monash Institute of Medical Engineering, Monash University, Melbourne. [4]National Vision Research Institute, Melbourne.
[#]tesler@student.unimelb.edu.au

978-1-4577-0220-4/16/$31.00 ©2016 IEEE

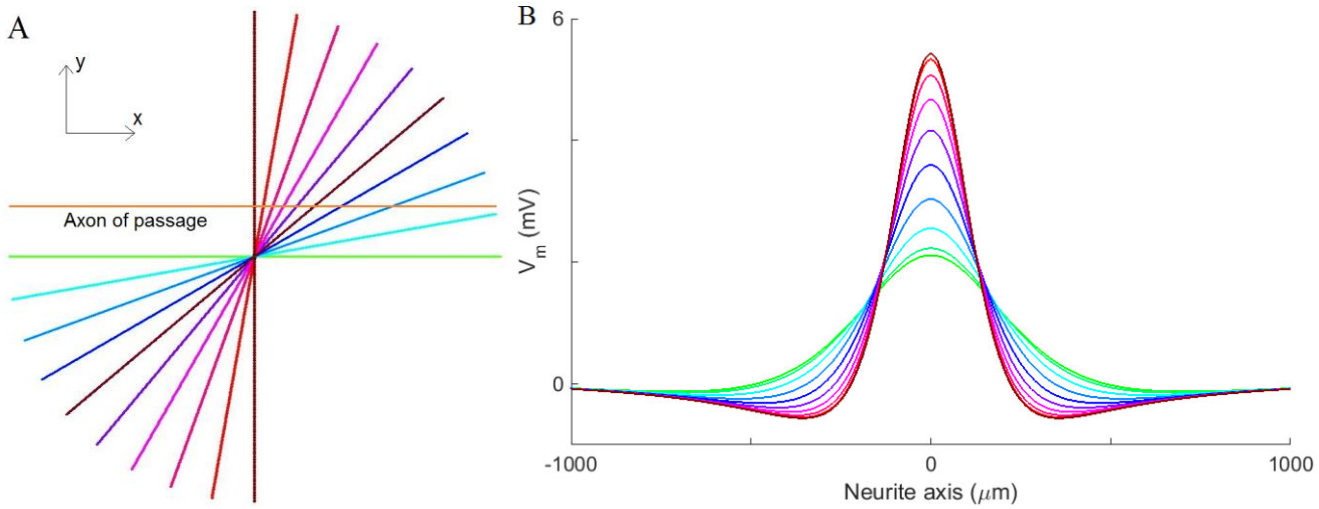

Figure 2: Geometry and calculated membrane potential from 4-layer retina simulations of neurites at a variety of x-y orientations with respect to the orientation of passing axons. (A) Simulation geometry showing an example of a parallel axon of passage orientation (orange) and of the neurites being considered in the ganglion cell layer (green-brown). (B) Membrane potential along neurites in the ganglion cell layer at the end of the cathodic phase (colors correspond to those in (A)).

calculated extracellular field or current density from the first stage as input into a more detailed model of a neuron to calculate membrane potential.

B. The four layer cellular composite model

The current approach uses a four layer description of retinal geometry for stage one of the volume conductor (Fig. 1). The flow of current in the extracellular space in each layer is described by a separate Poisson-type equation, allowing for differing tissue conductivities in each layer. The current delivered by disk electrodes enters as an explicit term on the right-hand-side of the continuity equation:

$$\begin{aligned} \nabla \cdot \mathbf{J}_{\mathrm{I}}(x,y,z,t) &= 0, \\ \nabla \cdot \mathbf{J}_{\mathrm{V}}(x,y,z,t) &= \sum_{\mathrm{i}}^{\mathrm{N}} \frac{I_{\mathrm{i}}(t)}{\pi {r_{\mathrm{i}}}^2} g_{r_{\mathrm{i}}}(x-x_{\mathrm{i}}, y-y_{\mathrm{i}}) \delta(z-z_{\mathrm{i}}), \\ \nabla \cdot \mathbf{J}_{\mathrm{N}}(x,y,z,t) &= 0, \\ \nabla \cdot \mathbf{J}_{\mathrm{G}}(x,y,z,t) &= 0, \end{aligned} \tag{1}$$

where $\mathbf{J}_\alpha$ is the extracellular current density in layer α, and each set of $(x_{\mathrm{i}}, y_{\mathrm{i}}, z_{\mathrm{i}}, r_{\mathrm{i}}, I_{\mathrm{i}}(t))$ represents the location, radius, and current stimulus of each of the N electrodes. The function $g_{r_{\mathrm{i}}}(\cdot)$ is the unit circular disk of radius r_{i}. I, V, N, and G correspond to insulator, vitreous, nerve fiber, and ganglion cell layers, respectively.

The constitutive equation is a generalized form of Ohm's Law for spatially and temporally dependent conductivity (i.e. admittivity),

$$\mathbf{J}_\alpha = \xi_\alpha(x,y,z,t) * \left(-\nabla \cdot \phi_\alpha(x,y,z,t)\right), \tag{2}$$

where ξ_α is the 3x3 admittivity kernel and ϕ_α is the extracellular potential of layer α. Boundary conditions are defined by equating potential and current density at layer boundaries.

Although not presented here for the sake of brevity, the solution of the system of partial differential equations defined by (1) and (2) at the layer boundaries can be obtained using Fourier domain methods, and yields expressions for the extracellular potential in each layer [7-10]. Specific layer conductivities define the level of anisotropy for each layer, as well as unique spatiotemporal dependencies. For the NFL and GCL, the form of the conductivity represents the assumed distribution of fiber orientations in each layer.

In the current work, the NFL is modeled as a parallel fiber bundle (anisotropic) and fibers in the GCL are modeled as having a uniform distribution of orientations (isotropic). The conductivity of the GCL (ξ_{G}), as for the conductivity of the insulator (ξ_{I}) and vitreous (ξ_{V}) layers, is described by an isotropic constant. The conductivity of the NFL (ξ_{N}) is captured by a non-local, non-instantaneous admittivity kernel provided by the cellular composite model [7,9] which is derived from an accurate characterization of the spatiotemporal electrical properties of individual neurites that comprise the tissue. This represents an improvement over typical volume conductor models, which assume tissue to be purely resistive, and are conflicted by internal model inconsistency between descriptions of extracellular and membrane potentials. In contrast, the cellular composite model employs an effective tissue admittivity which reflects cellular composition with respect to both geometric and physiological properties.

Stage two of the four layer model involves the calculation of the passive membrane potential in the neurite of interest, in either the NFL or the GCL. This is achieved using the neurite equations of Meffin et al. [7] which provide expressions for membrane activation due to both the longitudinal and transverse modes of current flow. In this work, the neurite equations have been generalized to allow for analysis of fibers with arbitrary x-y orientation using a 2-dimensional

rotation applied to the Fourier transform pairs of x and y in the Fourier domain.

III. Results

A. Effect of neurite orientation

To establish a basis for orientation-dependent axonal activation, the membrane potential for fibers in the GCL with different of orientations were compared (Fig 2). For this and all subsequent simulations, cathodic-first, biphasic pulse stimulus were used. A significant dependence on neurite orientation was observed, with a more than 2.5x increase in membrane activation for neurites oriented perpendicularly to axons in the NFL, when compared to parallel neurites.

B. Determination of membrane thresholds

In order to determine threshold potential values for the AIS and AOP, simulations were run which replicate the experimental procedures of Fried et al. [11]. By matching electrode geometry and location, neurite orientation, nerve fiber layer thickness and stimulation frequency, and by using experimentally determined threshold stimulus currents, the corresponding threshold membrane potentials for the axon initial segment and distal axon were calculated in the context of the current computational model. The calculated threshold potential values were 12.09 mV and 6.30 mV for the axon of passage and the axon initial segment, respectively.

C. Effect of electrode-retina separation and pulse duration

These threshold values were then used to determine whether given stimulus applications were effective in achieving preferential activation of the GCL over the NFL. A search of the pulse frequency, amplitude and electrode-retina separation parameter space was conducted. For each set of parameters, simulations were run to compare the membrane activation of parallel neurites in the NFL and neurites with a range of rotated orientations in the GCL. Under the assumption that the orientation of axon initial segments is described by a uniform distribution, the proportion of preferentially activated AIS fibers was determined. Here preferential activation is defined as when the membrane potential of an AIS reaches threshold potential at a lower stimulus current than is required to drive an AOP to threshold. Similar analyses have been conducted for a range of single and dual disk electrode configurations. For illustration, the case of two electrodes with equal stimuli is presented here (Fig. 3).

Of the pulse frequencies and electrode-retina separation distances tested, separation distance represented the dominant effect on preferential activation of the GCL for separations greater than 250 µm. For electrode separations of less than 250 µm, the interaction of both pulse frequency/duration and separation distance impacts on preferential activation. In general, larger separation distances lead to a higher proportion of preferentially activated AIS's, and for smaller separations, higher frequency stimulation is required for preferential activation.

IV. Discussion

The observed dependence on neurite orientation is a result of several competing factors. The dominant orientation of

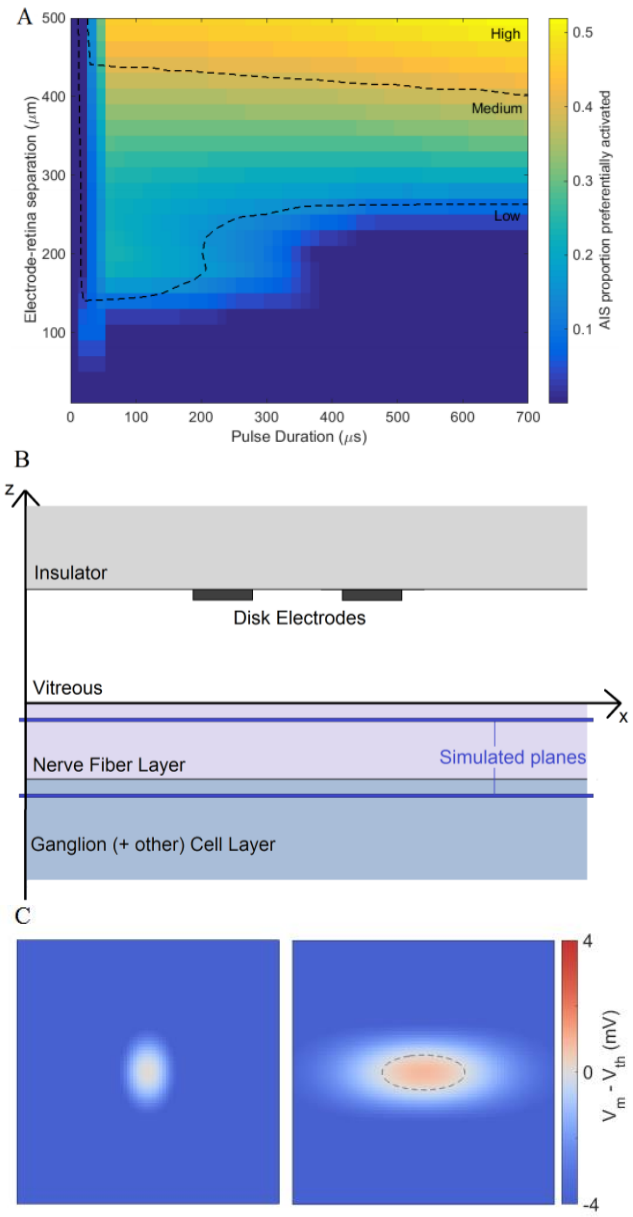

Figure 3: (A) Proportion of axon initial segment orientations preferentially activated for a range of electrode-retina separations and pulse durations, showing regions of low, medium and high stimulation selectivity (0-20%, 20-40%, and >40% respectively). Proportions are an approximation based on a 10° sampling of orientations from 0 to 90°. (B) Simulation geometry showing location of analysis planes. Examples of the indicated simulation planes are shown in (C). (C) Heat maps show an example of preferential activation (red) of perpendicular initial segments when stimulated with a pulse duration of 300 µs by electrodes positioned 400 µm above the retina. The colorbar shows the 'distance' in mV from membrane threshold for each of the NFL (left) and GCL (right), which represents the relative level of activation for axons of passage and axon initial segments, respectively.

axons in the NFL results in highly anisotropic spread of current under stimulation. For a given stimuli from a single electrode, the spread of the electric field will be greatest in the direction of the dominant NFL orientation. The magnitude of the consequent membrane activation is roughly proportional to the second derivative of the extracellular potential [12]. Due to these factors, the orientation of fibers in the GCL with respect to this anisotropy influences

membrane potential. Further, it is expected, and has been demonstrated in this work, that neurites oriented perpendicularly with respect to overlying axons are maximally activated via changes in the second spatial derivative of the extracellular potential. Intuitively, this is due to the fact that the reduced spread of potential along the perpendicular axis corresponds to a more rapid change in potential and hence a larger second derivative in that direction. The overall probability of eliciting a response selectively in the GCL then depends on the relative influence of fiber rotation, membrane threshold and fiber depth.

An important implication of the relationship between preferential activation and electrode separation is that there is likely to be a trade-off between the improvement in spatial selectivity achieved by having electrodes closer to the retina, and the likelihood of stimulation of passing axons. The analysis presented in this report implies that electrodes should be kept at least 150 μm away from the retina, and higher-frequency stimulation should be used. However, it may be that with more sophisticated stimulation strategies and multi-electrode geometries, preferential activation can be achieved for smaller electrode-retina distances. A key consideration will be whether or not typical electrode-retina separation distance fall in suitable ranges suggested by these results, and whether or not this can be controlled using more advanced implantation procedures or devices.

A challenge in experimentally validating results such as these is sensitivity of the result to the thickness of the NFL, which has significant variation across species. The human NFL is approximately 100 μm thick on average, whereas the NFL of mice and rats are approximately 20 μm and 40 μm, respectively. This may result in a dampening of the effects of orientation since the NFL is the primary source of anisotropy in the retina.

V. Conclusion

Although the current results are based on simulations of cylindrical neurites, the developed method for the analysis of arbitrarily rotated fibers can be applied directly to the simulation of unbranched axons with arbitrary morphology. A preliminary next step will be to validate the current results using ganglion cell axon reconstructions. A key point of interest will be whether or not the effect is sustained for spatially dynamic orientations. This will likely depend on the length constants associated with both axon curvature and membrane activation. In addition, results will be explored using Hodgkin-Huxley type membrane dynamics.

In order to translate these results to more clinically applicable outcomes, simulations should subsequently be designed to assess the feasibility of achieving preferential activation of the GCL using realistic high-density electrode array geometries. This will aim to capture the situation faced by practitioners, who must endeavor to avoid activation of axons of passage given pre-defined electrode configurations, constraints on allowable stimulus waveforms, and fixed electrode-retina separation distances.

These preliminary results highlight and explore the potential to achieve targeted epiretinal stimulation of the GCL whilst avoiding activation of axons in the NFL. Through a grid search of the pulse duration and electrode separation parameter space, the set of predicted stimulation conditions likely to achieve preferential stimulation has been determined. By more accurately modeling the effects of anisotropy and complex spatiotemporal interactions in retinal tissue, we have highlighted the potential to improve the resolution of epiretinal prostheses through control of stimulation parameters and electrode geometries.

VI. Acknowledgments

The authors acknowledge support under the Australian Research Council's Discovery Projects funding scheme (project number DP140104533). This research was supported by Victorian Life Sciences Computation Initiative (VLSCI) grant number VR0138 on its Peak Computing Facility at the University of Melbourne, and initiative of the Victorian Government.

References

[1] P. Werginz, S. Fried and F. Rattay, "Influence of the sodium channel band on retinal ganglion cell excitation during electric stimulation - a modeling study," *Neuroscience,* vol. 266, pp. 162-177, 2014.

[2] J. D. Weiland., M. S. Humayun, G. Dagnelie, E. De Juan, R. J. Greenberg and N. T. Iliff, "Understanding the origin of visual percepts elicited by electrical stimulation of the human retina," *Graefes Arch. Clin. Exp. Ophthalmol.,* vol. 237, no. 12, pp. 1007-1013, 1999.

[3] F. Rattay, L. P. Paredes and R. N. Leao, "Strength-duration relationship for intra- versus extracellular stimulation with microelectrodes," *Neuroscience,* vol. 214, pp. 1-13, 2012.

[4] J. F. Rizzo, J. Wyatt, J. Loewenstein, S. Kelly and D. Shire, "Methods and perceptual thresholds for short-term electrical stimulation of human retina with microelectrode arrays," *Invest. Ophthalmol. Vis. Sci.,* vol. 44, no. 12, pp. 5355-5561, 2003.

[5] F. Rattay and S. Resatz, "Effective electrode configurationfor selective stimulation with inner eye prostheses," *IEEE Trans. Biomed. Eng.,* vol. 51, no. 9, pp. 1659-1664, 2004.

[6] R. J. Greenberg, T. J. Velte, M. S. Humayun, G. N. Scarlatis and E. De Juan, "A computational model of electrical stimulation of the retinal ganglion cell," *IEEE Trans. Biomed. Eng.,* vol. 46, no. 5, pp. 505-514, 1999.

[7] H. Meffin, B. Tahayori, D. B. Grayden and A. N. Burkitt, "Modeling extracellular electrical stimulation: I. Derivation and interpretation of neurite equations," *J. Neural Eng.,* vol. 9, no. 6, 2012.

[8] B. Tahayori, H. Meffin, S. Dokos, A. N. Burkitt and D. B. Grayden, "Modeling extracellular electrical stimulation: II. Computational validation and numerical results," *J. Neural Eng.,* vol. 6, 2012.

[9] H. Meffin, B. Tahayori, E. N. Sergeev, I. M. Y. Mareels, D. B. Grayden and A. N. Burkitt, "Modelling extracellular electrical stimulation: III. Derivation and interpretation of neural tissue equations," *J. Neural Eng.,* vol. 11, no. 6, p. 065004, 2014.

[10] B. Tahayori, H. Meffin, E. N. Sergeev, I. M. Y. Mareels, A. N. Burkitt and D. B. Grayden, "Modelling extracellular electrical stimulation: IV. Effect of cellular composition of neural tissue on its spatio-temporal filtering properties," *J. Neural Eng.,* vol. 11, no. 6, p. 065005, 2014.

[11] S. I. Fried, A. C. W. Lasker, N. J. Desai, D. K. Eddington and J. F. Rizzo, "Axonal Sodium-Channel Bands Shape the Response to Electric Stimulation in Retinal Ganglion Cells," *J. Neurophysiol.,* vol. 101, no. 1, pp. 1972-1987, 2009.

[12] F. Rattay, "The basic mechanism for the electrical stimulation of the nervous system," *Neuroscience,* vol. 89, no. 2, pp. 335-346, 1999.